Mechanism Elucidation by EXAFS

Time Scale and Elementary Steps of CO-Induced Disintegration of Surface Rhodium Clusters**

*Akane Suzuki, Yasuhiro Inada, Aritomo Yamaguchi, Teiji Chihara, Makoto Yuasa, Masaharu Nomura, and Yasuhiro Iwasawa**

While the reaction kinetics and dynamics of molecules adsorbed on catalyst surfaces have been extensively studied, little is known about the dynamic structural change of active

[*] Prof. Dr. Y. Iwasawa, A. Suzuki
Department of Chemistry
Graduate School of Science
the University of Tokyo
Hongo, Bunkyo-ku, Tokyo, 113-0033 (Japan)
Fax: (+81) 3-5800-6892
E-mail: iwasawa@chem.s.u-tokyo.ac.jp

Dr. Y. Inada
Graduate School of Science
Nagoya University
Chikusa, Nagoya (Japan)

Dr. A. Yamaguchi, Prof. Dr. M. Yuasa
Faculty of Science and Technology
Tokyo University of Science
Noda, Chiba (Japan)

Dr. T. Chihara
RIKEN
Wako, Saitama 351-01 (Japan)

Prof. Dr. M. Nomura
Photon Factory
Institute of Materials Structure Science, KEK
Ibaraki 305-0801 (Japan)

[**] This study was supported by a Grant-in-aid for The 21st Century COE Program for Frontiers in Fundamental Chemistry from the Ministry of Education, Culture, Sports, Science and Technology.

Supporting information for this article is available on the WWW under http://www.angewandte.org or from the author.

 DOI: 10.1002/ange.200352318

metal sites in supported metal cluster/nanoparticle catalysts, such as the time scale of formation and disintegration of the active structure induced by reaction gases and the sequence of bond rearrangements involved in the dynamic event on the surfaces. The in situ time-resolved structural characterization of surface metal clusters and nanoparticles by energy-dispersive X-ray absorption fine structure (DXAFS) is essential to document their dynamic property on an atomic basis, which has been a long-term challenge to be addressed. We have succeeded in observing the CO-induced disintegration process of Rh clusters on an Al_2O_3 surface by DXAFS every 100 ms. Previous static studies on the similar surface phenomenon have been performed by IR,[1–3] XAFS,[4,5] and STM,[5,6] which revealed the structural modification of highly dispersed Rh nanoparticles/Al_2O_3 catalysts that leads to the formation of isolated $Rh(CO)_2$ species by CO adsorption. The DXAFS technique has been developed and improved to provide in situ structural information on dispersed catalytic materials at a time resolution of 1 s—several 10 s.[7–25] Herein, we report novel issues found by the time-resolved DXAFS characterization of the structural disintegrity of Rh clusters on an Al_2O_3 surface, namely, the time scale and sequence of dynamic bond rearrangements in the clusters and at the interface.

Figure 1 shows XANES (XANES = X-ray absorption near-edge spectroscopy) spectra at the Rh Kedge during the carbonylation process of the Rh/Al_2O_3 catalyst under 26.7 kPa of CO at 298 K. The DXAFS spectra were recorded

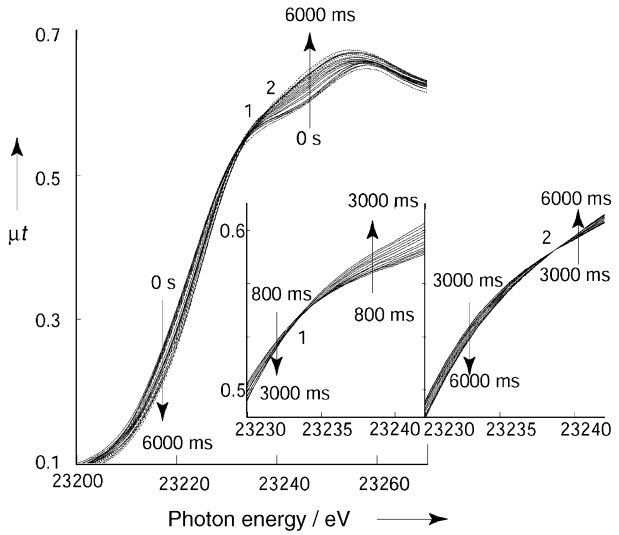

Figure 1. A series of XANES spectra at the Rh *K* edge during the carbonylation of Rh/Al_2O_3 under CO (26.7 kPa) at 298 K. The acquisition time of each spectrum is 100 ms, Cat.weight (wafer) = 80 mg.

every 100 ms. There is an isosbestic point at 23.234 keV (point **1**) in the serial XANES spectra during the period of 0.8–3 s as shown in the inset of Figure 1, thus indicating a direct change from a Rh species to another Rh species in its time scale. The spectra at the beginning of CO adsorption (0–600 ms) did not pass the isosbestic point. The k^3-weighted EXAFS oscillations at the Rh K edge during the carbonylation process are shown in Figure 2a. The amplitude of extended X-ray absorption fine structures (EXAFS) oscillations did not change significantly at 0–600 ms, but a remarkable decrease in the amplitude in the higher k range was observed from 600 ms till 3000 ms. This indicates that the observation of the isosbestic point is due to a structural change in the Rh clusters. The second isosbestic point was observed at

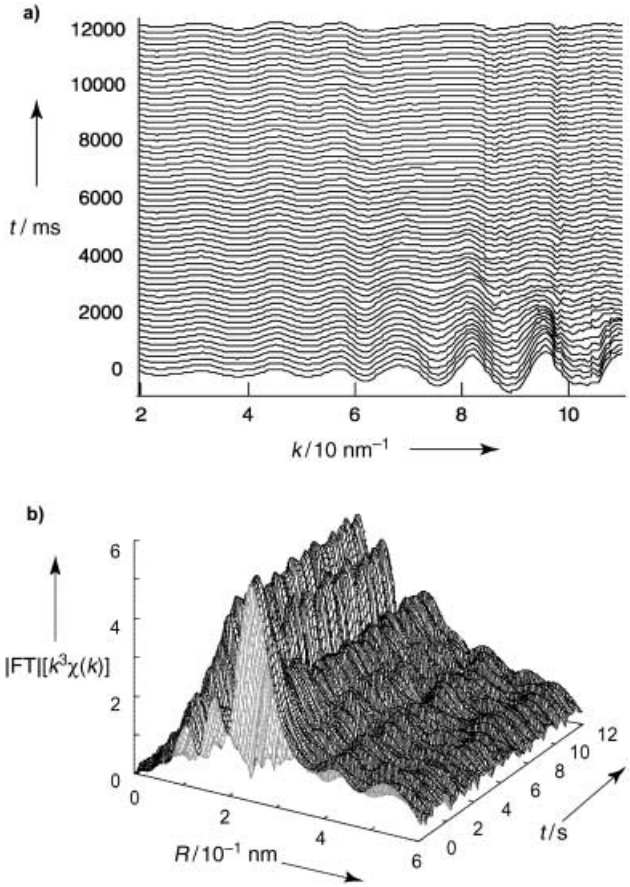

Figure 2. a) The k^3-weighted EXAFS oscillations and b) their Fourier transformed functions for Rh/Al_2O_3 at the Rh K-edge during the carbonylation process at 298 K measured by DXAFS every 100 ms.

23.239 keV (point **2**) after 3 s as shown in the inset of Figure 1. The existence of the isosbestic point different from the first one means that another structural change occurred as a sequential process during the period of 3–6 s. Two distinct peaks in the FT at 0.174 and 0.248 nm (phase-shift uncorrected), which are assigned to Rh–O and Rh–Rh, respectively, were observed at $t = 0$ as shown in Figure 2b. After CO adsorption an FT peak due to the formation of the Rh–C–(O) bond appeared at 0.123 nm (phase-shift uncorrected) within the first 200 ms, while the FT peaks for Rh–O and Rh–Rh remained unchanged over 600 ms. A drastic change in the FT was observed at 800–3000 ms, and the Rh–Rh peak completely disappeared at 3000 ms. The quality of the DXAFS spectra observed every 100 ms was good enough for the structural analysis. The values of the coordination numbers (C.N.) and bond length (R) determined by the curve fitting

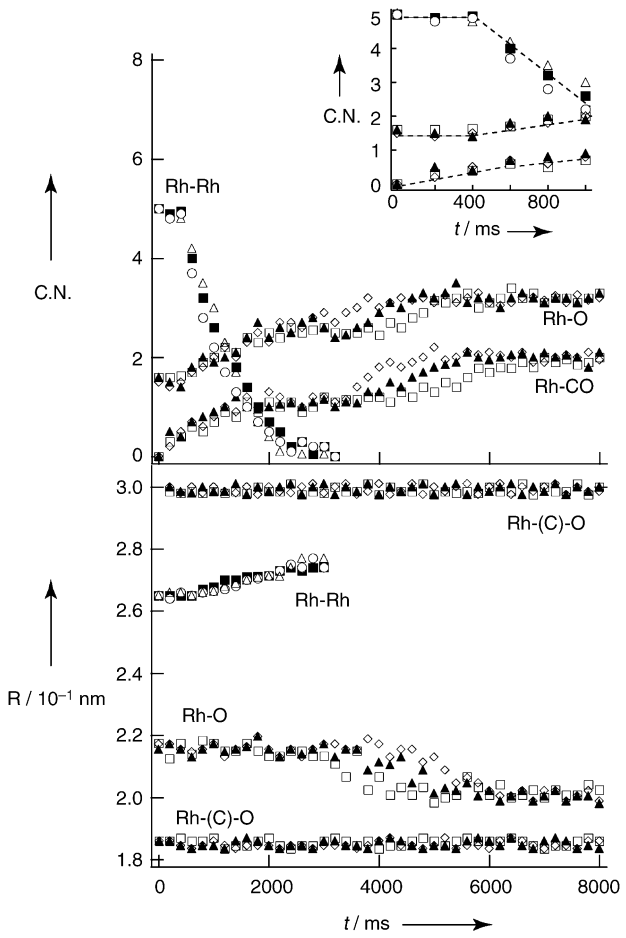

Figure 3. The values of coordination number (C.N.) and bond length (*R*) determined by the curve fitting as a function of CO exposure time at 298, 333, and 353 K. 298 K: Rh-Rh 298 (■), 333 (△), 353 (○); Rh-CO 298(□), 333 (▲), 353 (◇); Rh-O 298 (□), 333 (▲), 353 (◇).

Table 1: Structural parameters for the 2 wt% Rh/γ-Al_2O_3 catalyst.[a]

abs.-scat	C.N.	*R* [10^{-1} mm]	σ^2 [10^{-2} nm^2]
(Species A) after reduction at 593 K (flow of H_2) (0 s)			
($\Delta E_0 = 2.6$ eV, $R_f = 2.8\%$, *R* range = 0.15–0.3 nm)			
Rh-Rh	5.0 ± 0.4	2.65 ± 0.02	6.7 ± 0.2
Rh-O	1.6 ± 0.5	2.13 ± 0.02	13.7 ± 1
(Intermediate B) CO adsorption at 298 K (600 ms)			
($\Delta E_0 = 2.4$ eV, $R_f = 30\%$, *R* range = 0.10–0.32 nm)			
Rh-Rh	5.0 ± 0.4	2.65 ± 0.02	6.7 ± 0.2
Rh-O	1.6 ± 0.5	2.12 ± 0.02	13.7 ± 2
Rh-C	0.7 ± 0.6	1.85 ± 0.03	8.0 ± 3
Rh-(C)-O	0.7 ± 0.6	3.00 ± 0.04	9.7 ± 3
(Intermediate C) CO adsorption at 298 K (300 ms)			
($\Delta E_0 = 2.8$ eV, $R_f = 4.8\%$, *R* range = 0.10–0.32 nm)			
Rh-O	2.5 ± 0.5	2.13 ± 0.03	10.9 ± 2
Rh-C	1.2 ± 0.6	1.86 ± 0.03	8.0 ± 3
Rh-(C)-O	1.2 ± 0.6	2.99 ± 0.04	9.7 ± 3
(Species D) adsorption at 298 K (7000 ms)			
($\Delta E_0 = 1.8$ eV, $R_f = 4.5\%$, *R* range = 0.10–0.32 nm)			
Rh-O	3.2 ± 0.5	2.00 ± 0.03	10.9 ± 2
Rh-C	1.9 ± 0.6	1.87 ± 0.03	8.0 ± 3
Rh-(C)-O	1.9 ± 0.6	3.00 ± 0.04	9.7 ± 3

[a] **A** after reduction at 593 K (flow of H_2), and three intermediate **B, C** and **D** during CO adsroption at 298 K by DXAFS (see Figure 4).

were plotted as a function of CO exposure time at 298, 333, and 353 K in Figure 3. There were no changes in the Rh–Rh and Rh–O parameters at 0–600 ms, but the C.N. values for Rh–CO increased from 0 to 0.7 at 600 ms. After the interval of 600 ms, the C.N. of Rh–Rh bond decreased uniformly during the period of 800–3000 ms, accompanied by elongation of the Rh–Rh bond length and an increase of the C.N. for Rh–O from 1.6 to 2.5 at 3000 ms. The C.N. values for Rh–O and Rh–CO were almost constant at 2000–3000 ms, thus indicating the existence of a semistable structural state for CO-adsorbed Rh clusters on Al_2O_3. After 3000 ms the C.N. for Rh–O increased from 2.5 to 3.2 and for Rh–CO from 1.2 to 1.9 as shown in Figure 3; the *R* of Rh–O also decreased from 0.213 to 0.200 nm. The rate of the change was greater with an increase temperature. The observed and fitted FTs for the samples at 0 ms, 600 ms, 3000 ms, and 7000 ms are shown in the Supporting Information and the determined structural parameters are given in Table 1. The change in the C.N. values determined by the DXAFS analysis was in excellent accordance with the result of volumetric measurements (see Supporting Information); the amount of adsorbed CO molecules is plotted as a function of CO exposure time at 298 K.

Thus the time-resolved DXAFS analysis reveals three elementary steps for the surface dynamic structural rearrangement of Rh clusters involving two intermediate states as depicted in Figure 4. Before CO exposure ($t = 0$) Rh atoms in

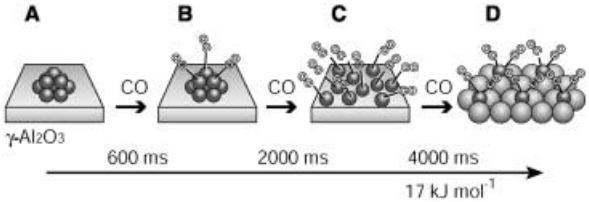

Figure 4. An illustrative mechanism, with times given as taken from the beginning of the reaction, of three elementary steps at 298 K for the disintegration of Rh clusters on Al_2O_3 during CO adsorption by time-resolved DXAFS.

the cluster interact with the surface oxygen atoms of Al_2O_3 at the distance of 0.213 nm. The C.N. (5.0) and *R* (0.265 nm) of Rh–Rh (Table 1) are in good agreement with those determined by conventional XAFS (4.9 and 0.264 nm). These structural parameters assume that the Rh cluster consists of seven atoms in the first layer and three atoms in the second layer as shown in Figure 4, which shows the C.N. of 5.4 for Rh–Rh bond. The C.N. value of 1.6 for Rh–O indicates that each Rh atom in the lower layer interacts with two O atoms of the Al_2O_3 surface. At the first step of the dynamic processes (0–600 ms) CO rapidly adsorbs on the Rh cluster to give a C.N. of 0.7 for Rh–CO, which indicates that one CO molecule adsorbs on each Rh atom of the second layer. At this stage no Rh–Rh bond breaking occurs. At the second step after 600 ms the Rh–Rh bonds become weaker by further CO adsorption and the Rh cluster is completely disintegrated at 3000 ms, at which point the ratio of adsorbed CO to Rh is one (see

Supporting Information). The existence of the isosbestic point (**1**) in Figure 1 indicates that the second step consists of a one-to-one direct conversion, namely from $[Rh_{10}(CO)_3]$ (**B**) to $[Rh{-}CO]_{10}$ (**C**) in Figure 4. The [Rh–CO] can migrate across the Al_2O_3 surface to react with OH groups. The fragmentation of the Rh cluster permits the adsorption of further CO molecules on the Rh atoms at the third step (3000–6000 ms) to form $[Rh(CO)_2]$, which interacts with three surface O atoms as shown in Figure 4. This process is also a direct transformation process as evidenced by the second isosbestic point (**2**), in which the Rh atoms more strongly interact with the surface because of a decrease in the Rh–O distance from 0.213 to 0.200 nm (Table 1). The $[Rh(CO)_2]$ monomers form on the Cl-free Rh/Al_2O_3 catalyst, which is in contrast to the situation previously reported.[26]

The [Rh–CO] species and the $[Rh(CO)_2]$ species were also confirmed by in situ FTIR. The FTIR spectra were recorded as difference spectra on a JASCO FTIR 230 spectrometer in a transmission mode. In FTIR spectra (see Supporting Information) a peak at 2060 cm^{-1} is assigned to ν_{CO} for a terminal CO molecule on a Rh atom, while two peaks around 2095 and 2023 cm^{-1} are assigned to symmetric and asymmetric ν_{CO} for Rh discarbonyl species. After the 1.5 s CO exposure, the peak intensity at 2060 cm^{-1} increased at first, followed by the development of peaks at 2095 and 2023 cm^{-1} (4.5 s). Only these two bands were observed at 10.5 s. The formation of Rh dicarbonyl species is in accordance with the previous reports.[1–3]

We have carried out the DXAFS measurements at three different temperatures. The rates of the first and second steps were independent of the temperature at the present conditions. In contrast, the rate of the third step clearly depended on the temperature and the activation energies were estimated to be 15 ± 2, 17 ± 2, and 19 ± 2 kJ mol^{-1} for the changes in the C.N. of Rh–CO, the C.N. of Rh–O, and the *R* of Rh–O, respectively, which are in good agreement with each other. By CO adsorption, the Rh–Rh bond distance increased from 0.26 nm for the incipient Rh clusters to 0.27 nm for the $[Rh{-}CO]_{10}$ species, while the Rh cluster framework disintegrated during the Rh–Rh elongation. Thus the [Rh–CO] species can move off from the cluster at the surface without any significant energy barrier. The slowest step in the cluster disintegration with the energy barrier of 17 kJ mol^{-1} is the formation of $[Rh(CO)_2]$ monomers, which occurs concertedly with the bond rearrangement (C.N. and *R* of Rh–O) at the interface and probably with the oxidation of Rh^0 to Rh^+ by surface OH groups.

In summary we have shown the time scale and bond sequence in the dynamic structural disintegration of Rh clusters on the γ-Al_2O_3 surface, which proceeds through two intermediate states and is detected by time-resolved DXAFS every 100 ms. The present time-resolved structural analysis provides crucial structural aspects to elucidate the mechanism for dynamic surface processes and contributes to a new area of structural dynamics of metal clusters/nanoparticles dispersed at surfaces.

Experimental Section

A 2 wt% Rh/γ-Al_2O_3 catalyst was prepared by an incipient wet-impregnation method with an aqueous solution of $RhCl_3 \cdot 3H_2O$, followed by drying at 393 K for 30 h to remove the solvent. The obtained sample of 80 mg was pressed to a disk (4 mmϕ) and placed at a holder of an in situ DXAFS cell, and reduced at 613 K for 1.5 h under a flow of hydrogen, followed by evacuation at 573 K for 1 h. It is noteworthy that the amount of residual Cl in the Rh/Al_2O_3 sample was below detection limits by XRF and elemental analysis.

DXAFS measurements in the energy range 23.0–24.2 keV were carried out at BL-9C in KEK-PF. A four-point supporting crystal bender was newly developed for a Si(311) bent-crystal polychromator (Bragg-type) to obtain elliptical optics for focusing incident X-rays on the sample. A self-scanning photodiode array (PDA: 1024 sensing elements: 25 μm width and 2.5 mm height for each element) manufactured by HAMAMATSU Photonics (S3904-1024FX SPL3402) was used as a position-sensitive linear detector. A fiber optical plate embrocated by a CsI(Tl) fluorescent was directly coupled at the active area of PDA to convert X-ray to visible light. The energy calibration at each sensing element of the PDA was performed by comparison with an XAFS spectrum of a Rh foil recorded by using an Si(311) channel-cut monochromator. The in situ DXAFS cell was made of stainless steel and had two slit windows with capton films to measure the incident and transmitted X-rays. The obtained XAFS spectra were analyzed by using the UWXAFS program.[27] After the background subtraction by the AUTOBK program,[28] the Fourier transformation for the k^3-weighted EXAFS oscillation was performed, and the structural parameters were determined by a curve fitting procedure in the *R* space by using the FEFFIT program involving multiple scattering effects.[29] The back scattering amplitude and phase shift functions, and the mean free paths were generated by the FEFF8 code that accounted for energy resolution of the DXAFS spectrometer (4.0 eV). The time-resolved DXAFS spectra were fitted by using a model function composed of four shells, that is, Rh–C–(O) and Rh–(C)–O for carbonyl ligands, Rh–Rh for Rh clusters, and Rh–O at the interface between the Rh cluster and the Al_2O_3 surface. The coordination numbers of Rh–C–(O) and Rh–(C)–O bonds were fixed to be the same. The Debye–Waller factors of all the contributions were fixed at the values obtained by conventional XAFS to reduce the number of independent parameters in the fitting procedure.[30] The validity of this procedure was confirmed for stable Rh species by comparing the Debye–Waller factors obtained by the DXAFS and conventional XAFS. The residual factors for the fitting were typically 4%.

Received: July 8, 2003 [Z52318]
Published Online: September 25, 2003

Keywords: EXAFS spectroscopy · heterogeneous catalysis · reaction mechanisms · solid-state structures · time-resolved spectroscopy

[1] A. C. Yang, C. W. Garland, *J. Phys. Chem.* **1957**, *61*, 1504.
[2] R. R. Cavanagh, T. Yates, Jr., *J. Chem. Phys.* **1981**, *74*, 4150.
[3] P. Basu, D. Panayotov, J. T. Yates, Jr., *J. Am. Chem. Soc.* **1988**, *110*, 2074.
[4] H. D. J. van't Blik, J. B. A. D. van Zon, T. Huizunga, J. C. Koningsberger, R. Prins, *J. Am. Chem. Soc.* **1985**, *107*, 11; H. D. J. van't Blik, J. B. A. D. van Zon, T. Huizunga, J. C. Koningsberger, R. Prins, *J. Am. Chem. Soc.* **1985**, *107*, 3140.
[5] A. Berko, G. Menesi, F. Solymosi, *J. Phys. Chem.* **1996**, *100*, 17732.
[6] A. Berko, F. Solymosi, *J. Catal.* **1999**, *183*, 91.
[7] T. Matsushita, R. P. Phizackerley, *Jpn. J. Appl. Phys.* **1981**, *20*, 2223.

[8] A. M. Flank, A. Fontaine, A. Jucha, M. Lemonnier, C. Williams, *J. Phys. Lett.* **1982**, *43*, L315.
[9] D. Bazin, H. Dexpert, P. Lagarde, P. Bournonville, *J. Catal.* **1988**, *110*, 209.
[10] A. Fontaine, E. Dartyge, J. P. Itie, A. Jucha, A. Polian, H. Tolentino, G. Tourillon, *Top. Curr. Chem.* **1989**, *151*, 179.
[11] J. W. Couves, J. M. Thomas, D. Waller, R. H. Jones, A. J. Dent, G. E. Derbyshire, G. N. Greaves, *Nature* **1991**, *354*, 465.
[12] G. Sanker, J. M. Thomas, D. Waller, J. W. Couves, C. R. A. Catlow, G. N. Greaves, *J. Phys. Chem.* **1992**, *96*, 7485.
[13] T. Ressler, M. Hagelstein, U. Hatje, W. Metz, *J. Phys. Chem. B* **1999**, *101*, 6680.
[14] N. Hilbrandt, R. Frahm, M. Martin, *J. Phys. IV* **1997**, *7*, 727.
[15] S. G. Fiddy, M. A. Newton, A. J. Dent, G. Salvini, J. M. Corker, S. Turin, T. Campbell, J. Evans, *Chem. Commun.* **1999**, 851.
[16] A. Yamaguchi, T. Shido, Y. Inada, T. Kogure, K. Asakura, M. Nomura, Y. Iwasawa, *Catal. Lett.* **2000**, *68*, 139.
[17] A. Yamaguchi, A. Suzuki, T. Shido, Y. Inada, K. Asakura, M. Nomura, Y. Iwasawa, *Catal. Lett.* **2001**, *71*, 203.
[18] A. Yamaguchi, T. Shido, Y. Inada, T. Kogure, K. Asakura, M. Nomura, Y. Iwasawa, *Bull. Chem. Soc. Jpn.* **2001**, *74*, 801.
[19] S. G. Fiddy, M. A. Newton, C. T. Campbell, J. M. Corker, S. Turin, J. Evans, A. J. Dent, I. Harvey, G. Salvini, *Chem. Commun.* **2001**, 445.
[20] M. A. Newton, D. G. Burnaby, A. J. Dent, S. Diaz-Moreno, J. Evans, S. G. Fiddy, T. Neisius, S. Pascaralli, S. Turin, *J. Phys. Chem. A* **2001**, *105*, 5965.
[21] A. Yamaguchi, A. Suzuki, T. Shido, Y. Inada, K. Asakura, M. Nomura, Y. Iwasawa, *J. Phys. Chem. B* **2002**, *106*, 2415.
[22] M. A. Newton, A. J. Dent, S. Diaz-Moreno, S. G. Fiddy, J. Evans, *Angew. Chem.* **2002**, *114*, 2699; *Angew. Chem. Int. Ed.* **2002**, *41*, 2587.
[23] A. J. Dent, *Top. Catal.* **2002**, 27.
[24] C. Lamberti, C. Prestipino, F. Bonino, L. Capello, S. Bordiga, G. Spoto, A. Zecchina, S. Diaz-Moreno, B. Cremaschi, M. Garilli, A. Marsella, D. Carmello, S. Vidotto, G. Leofanti, *Angew. Chem.* **2002**, *114*, 2447; *Angew. Chem. Int. Ed.* **2002**, *41*, 2341.
[25] F. Meneau, G. Sankar, N. Morgante, R. Winter, C. R. A. Catlow, G. N. Greaves, J. M. Thomas, *Faraday Discuss.* **2003**, *122*, 203.
[26] P. Johnston, R. W. Joyner, *J. Chem. Soc. Faraday Trans.* **1993**, 863.
[27] E. A. Stern, M. Newville, B. Ravel, Y. Yacoby, D. Haskel, *Phys. B* **1995**, *208*, 117.
[28] M. Newville, P. Livins, Y. Yacoby, E. A. Stern, J. J. Rehr, *Phys. Rev. B* **1993**, *47*, 14126.
[29] A. L. Ankudinov, B. Ravel, J. J. Rehr, S. D. Conradson, *Phys. Rev. B* **1998**, *58*, 7565.
[30] E. A. Stern, *Phys. Rev. B* **1993**, *48*, 9825.

